The Journal of Immunology

RESEARCH ARTICLE | OCTOBER 28 2024

Identification of a Specific Granular Marker of Zebrafish Eosinophils Enables Development of New Tools for Their Study

Miriam Herbert; ... et. al

J Immunol ji2400259.
https://doi.org/10.4049/jimmunol.2400259

Identification of a Specific Granular Marker of Zebrafish Eosinophils Enables Development of New Tools for Their Study

Miriam Herbert,*,† Christian Goosmann,‡ Volker Brinkmann,‡ Christiane Dimmler,* and Mark R. Cronan*

Eosinophils control many aspects of the vertebrate innate immune response. They contribute to homeostasis, inflammatory conditions and defense against pathogens. With the varied functions of eosinophils, they have been found to play both protective and pathogenic roles in many diseases. The zebrafish (*Danio rerio*) has emerged as a useful model organism for human diseases but tools to study eosinophils in this model are severely limited. Here, we characterize a new and highly specific marker gene, *embp*, for eosinophils in zebrafish and report a new transgenic reporter line using this gene to visualize eosinophils in vivo. In addition, we created an Embp-specific polyclonal Ab that allows the identification of eosinophils ex vivo. These new tools expand the approaches for studying eosinophils in the zebrafish model. Using these reagents, we have been able to identify Embp as a constituent of eosinophil granules in zebrafish. These advances will allow for the investigation of eosinophil biology in the zebrafish model organism, allowing researchers to identify the contribution of eosinophils to the many diseases that are modeled within zebrafish and also shed light on the evolution of eosinophils within vertebrates. ***The Journal of Immunology*****, 2024, 213: 1–9.**

Zebrafish (*Danio rerio*) are an increasingly popular model organism in biomedical research and have been used to model a variety of human diseases (1–3). They possess an evolutionarily conserved vertebrate immune system containing all major cell types, including eosinophils (4). The zebrafish's naturally transparent larval stage, high fecundity, and genetic tractability make it an excellent model organism to study hematological and immunological questions (5,6). Although eosinophils are a recognized part of the zebrafish immune repertoire, the limited array of existing tools for the study of eosinophil function in zebrafish has restricted the use of this model for the study of eosinophil biology.

Eosinophils belong to the group of granulocytes and are characterized by large cytoplasmic granules that store a plethora of preformed signaling and effector molecules, which can be stained with acidic dyes such as eosin (7). They are well known effector cells in parasitic infections as well as mediators of allergic or inflammatory conditions (e.g. asthma). Although they are only found in low numbers under homeostatic conditions, they have been associated with both beneficial as well as detrimental effects in health and disease (8–10). However, their contributions often remain elusive.

Past work characterizing eosinophil responses in zebrafish have mostly relied on classical histological staining approaches and the transgenic *Tg*(*gata2:eGFP*) line (11). In this transgenic line, the *gata2a* promoter drives the expression of enhanced GFP (eGFP). Because eosinophils express this marker highly, this transgenic line can be used to isolate eosinophils using FACS. However, *gata2a* is not expressed exclusively in eosinophils and therefore this reporter line cannot be used to identify eosinophils in vivo.

The broad importance of eosinophils in a range of conditions as well as their evolutionary conservation highlight the critical role played by this cell type and the need for comprehensive methods to further investigate their function in a range of settings. In this study, we identify an eosinophil granule-specific marker in zebrafish that we use to create both a transgenic fluorescent reporter line as well as a polyclonal Ab to visualize zebrafish eosinophils both in vivo and ex vivo. We found that our eosinophil reporter line and Ab could be used to identify eosinophils in tissue as well as by flow cytometry, facilitating the study of this immune cell population. Using electron microscopy (EM), we found that this marker localizes specifically to eosinophil granules. To further demonstrate the utility of our tools, we visualized the localization of eosinophils to mycobacterial granulomas, validating the use of this marker during inflammatory conditions.

Materials and Methods

Zebrafish housing and breeding

Animals were housed and bred under standard conditions. All experiments were conducted in accordance with institutional (Max Planck Institute for Infection Biology), state (LAGeSo Berlin), and German ethical and animal

*In Vivo Cell Biology of Infection Group, Max Planck Institute for Infection Biology, Berlin, Germany; †Faculty of Life Science, Humboldt University of Berlin, Berlin, Germany; and ‡Microscopy Core Facility, Max Planck Institute for Infection Biology, Berlin, Germany

ORCIDs: 0000-0002-8732-4766 (M.H.); 0000-0003-4735-3682 (V.B.); 0000-0002-3760-1649 (M.R.C.).

Received for publication May 8, 2024. Accepted for publication October 9, 2024.

This work was supported by the Max Planck Society. In addition, M.H. is supported by the Add-On Fellowship of the Joachim Herz Foundation.

M.H. designed research, performed research, collected data, analyzed and interpreted data, performed statistical analysis, and wrote the manuscript; C.G. performed research, collected data, and analyzed and interpreted data; V.B. performed research, collected data, and analyzed and interpreted data; C.D. performed research and collected data; and M.R.C. designed research, performed research, collected data, analyzed and interpreted data, wrote the manuscript, and provided supervision.

Address correspondence and reprint requests to Dr. Mark R. Cronan, Max Planck Institute for Infection Biology, Charitéplatz 1, 10117 Berlin, Germany. E-mail address: cronan@mpiib-berlin.mpg.de

The online version of this article contains supplemental material.

Abbreviations used in this article: dpf, days postfertilization; EM, electron microscopy; embp, eosinophil most abundant protein; FFPE, formalin-fixed, paraffin-embedded; eGFP, enhanced GFP; h, human; IPEX, i.p. exudate; MBP-1, major basic protein 1; MBP-2, major basic protein 2; PAS, periodic acid–Schiff; PFA, paraformaldehyde; pI, isoelectric point; RT, room temperature; ToB, toluidine blue; WG, Wright–Giemsa; WKM, whole-kidney marrow.

https://doi.org/10.4049/jimmunol.2400259

welfare guidelines and regulations. Male and female animals were used in approximately the same ratios for all experiments.

Zebrafish lines

The wild-type strain in this study was *AB and all zebrafish strains used this background. The transgenic lines that were used in this study included *Tg*(*gata2:eGFP*)^{la3} (12) and *Tg*(*mpx:GFP*)^{i114} (13), which have been previously been described, and the newly created *TgKI*(*embp-tdTomato, cryaa:EGFP*)^{ber1} line, where *embp* stands for eosinophil most abundant protein (see below). Fluorescent reporter lines were maintained as heterozygotes.

Generation of transgenic zebrafish line

The new eosinophil reporter line was created using a CRISPR/Cas9 based knock-in approach inserting into a noncoding region as previously described (14). The transgenic insert used to generate *TgKI*(*embp-tdTomato,cryaa:EGFP*) zebrafish was assembled using the Golden Gate cloning system (15) as previously described (S. Hurst, C. Dimmler, M.R. Cronan, and M. Cronan, manuscript posted on bioRxiv, DOI: 10.1101/2024.08.02.606358). The insert combines the last two exons of *embp* (also known as *dkeyp75b4.10* or *eslec*, ENSDARG00000079043) amplified from bacterial artificial chromosome clone CH211-226G7 (BACPAC Genomics), a tdTomato sequence, followed by UbB poly(A) and a transgenesis marker encompassing the *cryaa* promoter (16) driving eGFP in the reverse orientation. The DNA donor fragment was PCR amplified and cleaned up prior to injection using the gel and PCR clean-up kit (Macherey-Nagel). One-cell-stage zebrafish embryos were injected with ∼1–2 nl of 2.5 ng/μl DNA donor fragment together with 12.5 ng/μl single-guide RNA targeting *embp* (targeting sequence: 5′-GGACAATTTTCATGACAAGA-3′, IDT) and 75 ng/μl Cas9 protein (IDT). At 3 d postfertilization (dpf) larvae were screened for GFP expression in the retina and raised to adulthood. Mosaic F_0 founders were outcrossed to *AB fish and screened for germline transmission of the transgenesis marker (GFP^+ eyes). GFP^+ F_1 fish were raised to adulthood and screened for $tdTomato^+$ eosinophils using flow cytometry at the age of ∼3–6 mo old.

Flow cytometry and cell sorting

Immune cells were isolated from whole-kidney marrow (WKM) and i.p. exudate (IPEX) in L-15 (Thermo Fisher Scientific) + 5% FCS as previously described (11). In brief, an incision was made on the ventral side of the fish and the peritoneal cavity was washed with 100 μl of L-15 + 5% FCS to collect IPEX cells. This process was repeated approximately three to four times to collect a sufficient number of cells. Next, the inner organs were removed and WKM was isolated as previously described (17). Single-cell suspensions were made using 100- and 40-μm cell strainers (VWR). The single-cell suspensions were centrifuged at 300 × *g* for 5 min at room temperature (RT) and resuspended in 1 ml of 1× PBS + 5% FCS. Cells were stained with DAPI (Thermo Fisher Scientific) for 15 min at RT before flow cytometric analysis. Flow cytometry was performed on a BD FACSCanto II (Becton Dickinson), and cell sorting was performed on a Sony MA900 cell sorter (Sony). Data were analyzed with FlowJo version 10.6.2. Dead cells, identified by DAPI staining, were excluded from the analysis, and gating was performed on single cells by using forward scatter and side scatter properties to exclude doublets.

Cytology

Cytospin preparations were carried out using a Cytospin3 (Shandon) centrifuge. Sorted eosinophils were resuspended in 150 μl of 1× PBS with 5% FCS. Cytospin chambers were prewetted with 100 μl of 5% FCS-PBS. The cells were then centrifuged at 800 rpm for 3 min at low acceleration. Slides were air-dried overnight at RT before fixation with 4% paraformaldehyde (PFA) in PBS and subsequent staining.

Zebrafish sectioning

Zebrafish were euthanized by hypothermic shock in ice-cold water. Subsequently, the fish were fixed in 4% PFA solution for 2 d at RT, decalcified in 0.35 M EDTA solution for 7 d, and paraffin embedded as previously described (18). Paraffin-embedded zebrafish were sectioned into 5-μm thin sections using a Microm HM355S rotary microtome (Thermo Fisher Scientific), floated onto Polysine slides (VWR), and dried at 37°C overnight.

Histological staining

Paraffin sections were deparaffinized in two changes of 100% xylene for 10 min each and then rehydrated in two changes of 100% EtOH, two changes of 95% EtOH, and one change each of 70% EtOH and 50% EtOH. Sections were washed with deionized water.

Histological staining was carried out according to the manufacturer's protocols (Sigma-Aldrich). Samples were mounted using DPX new mounting media (Sigma-Aldrich).

Immunofluorescence staining

Single-cell suspensions were obtained as described in *Flow cytometry and cell sorting*. Tissue sections were obtained as described under *Zebrafish sectioning* and deparaffinized as described in *Histological staining*. The *Mycobacterium marinum*–infected, paraffin-embedded zebrafish were a gift from David M. Tobin.

Single-cell suspensions were fixed with 4% PFA in PBS in a 96-well plate for 15 min at RT. After washing three times with 1× PBS, cells were permeabilized with 0.1% (v/v) Triton X-100/PBS for 15 min. Blocking was done with 3% goat serum/PBS for 1 h at RT, and subsequent primary Ab (Table I) staining was done in 3% goat serum/PBS overnight at 4°C. Cells were washed three times with 1× PBS and stained with secondary Ab (Table I) solution in 3% goat serum/PBS for 1 h at RT. Cells were washed again three times with 1× PBS and counterstained with DAPI (0.2 μg/ml). After a final wash with 1× PBS, cells were transferred to 50% (v/v) glycerol in 20 mM Tris mounting media for subsequent imaging.

For histology slides, Ag retrieval was performed by incubating deparaffinized slides in Ag retrieval solution of 10 mM Tris/1 mM EDTA (pH 9.0) followed by heat treatment in a pressure cooker (Krups) for 10 min. After cooling down to RT in Ag retrieval buffer, slides were blocked with 3% goat serum/PBS for 30 min and subsequently stained as described above. Selected samples were additionally treated with a Vector TrueVIEW autofluorescence quenching kit (Vector Laboratories) according to the manufacturer's protocol and mounted using the hard-curing mounting medium provided with the kit.

Microscopy

Color images of classical histological staining were acquired using a Leica DMR microscope and ProgRes SpeedXT core 3 camera (Jenoptik) or AxioScan Z1 (Zeiss).

Fluorescence images were taken on a Nikon Eclipse Ti2 microscope (Nikon) with a Dragonfly 200 confocal system (Oxford Instruments) and ×10, ×20, or ×40 objectives (Nikon). Image files were processed with Fiji ImageJ (19) and Zeiss Zen Blue (Zeiss).

Cryo-immunogold EM

Embp-$tdTomato^+$ eosinophils were isolated and sorted as described above. Cells were fixed with 4% PFA and 0.05% glutaraldehyde in PBS. The cells were harvested, gelatin-embedded, and infiltrated with 2.3 M sucrose according to the method described (20). Ultrathin sections were cut at −110°C with an RMC MTX/CRX cryo-ultramicrotome (Boeckeler Instruments, Tucson AZ) and transferred to carbon- and pioloform-coated EM grids and blocked with 0.3% BSA, 6 mM glycine, 3% cold washed fish gelatine in PBS. The sections were incubated with appropriate dilutions in the same buffer of rabbit polyclonal Ab directed against Embp (Table I) and chicken mAb against mCherry (Table I). Secondary Ab incubations were carried out with goat anti-rabbit or anti-chicken Abs coupled to 12- or 6-nm gold particles, respectively (Jackson ImmunoResearch, West Grove, PA). Specimens were then contrasted and embedded with uranyl-acetate/methylcellulose following the method described before (21) and analyzed in a Leo 912AB transmission electron microscope (Zeiss, Oberkochen, Germany) at 120 kV acceleration voltage. Micrograph mosaics were scanned using a bottom mount Cantega digital camera (SIS, Münster, Germany) with ImageSP software from TRS (Tröndle, Moorenweis, Germany). Images were processed with FigureJ (22) in Fiji ImageJ.

Statistical analysis

All experiments were repeated at least three times independently. Group sizes and statistical tests used are indicated in the figures and figure legends. Statistical tests were performed and visualized using Prism 9 (GraphPad).

Data availability

For original data or access to the novel transgenic line, please contact the corresponding author.

Results

Embp is a granular marker for zebrafish eosinophils

Previous studies into zebrafish eosinophils have often used broadly expressed markers, like the *Tg*(*gata2:eGFP*) line, or histological properties to identify eosinophils. Single cell RNA-Seq (scRNA-Seq) data

allow clustering and annotation of cell types based on transcriptomic profiles. These analyses facilitate an unbiased investigation into uncharacterized gene expression patterns. Using previously published zebrafish scRNA-Seq data sets (GSE161712 [23], GSE112438 [24]), we searched for differentially and highly expressed genes in eosinophil populations. One gene that stood out was *dkeyp75b4.10* (also known as *eslec*), a previously uncharacterized protein with a C-type lectin domain that is highly and differentially expressed in eosinophils. Ranked by gene expression, *dkeyp75b4.10* is the most abundant protein coding transcript in the eosinophil population (Fig. 1A). A recent report established that the promoter of this gene is eosinophil-lineage specific (25). Based on these findings and our results described below, we have renamed this gene *embp*, which we use throughout for clarity purposes.

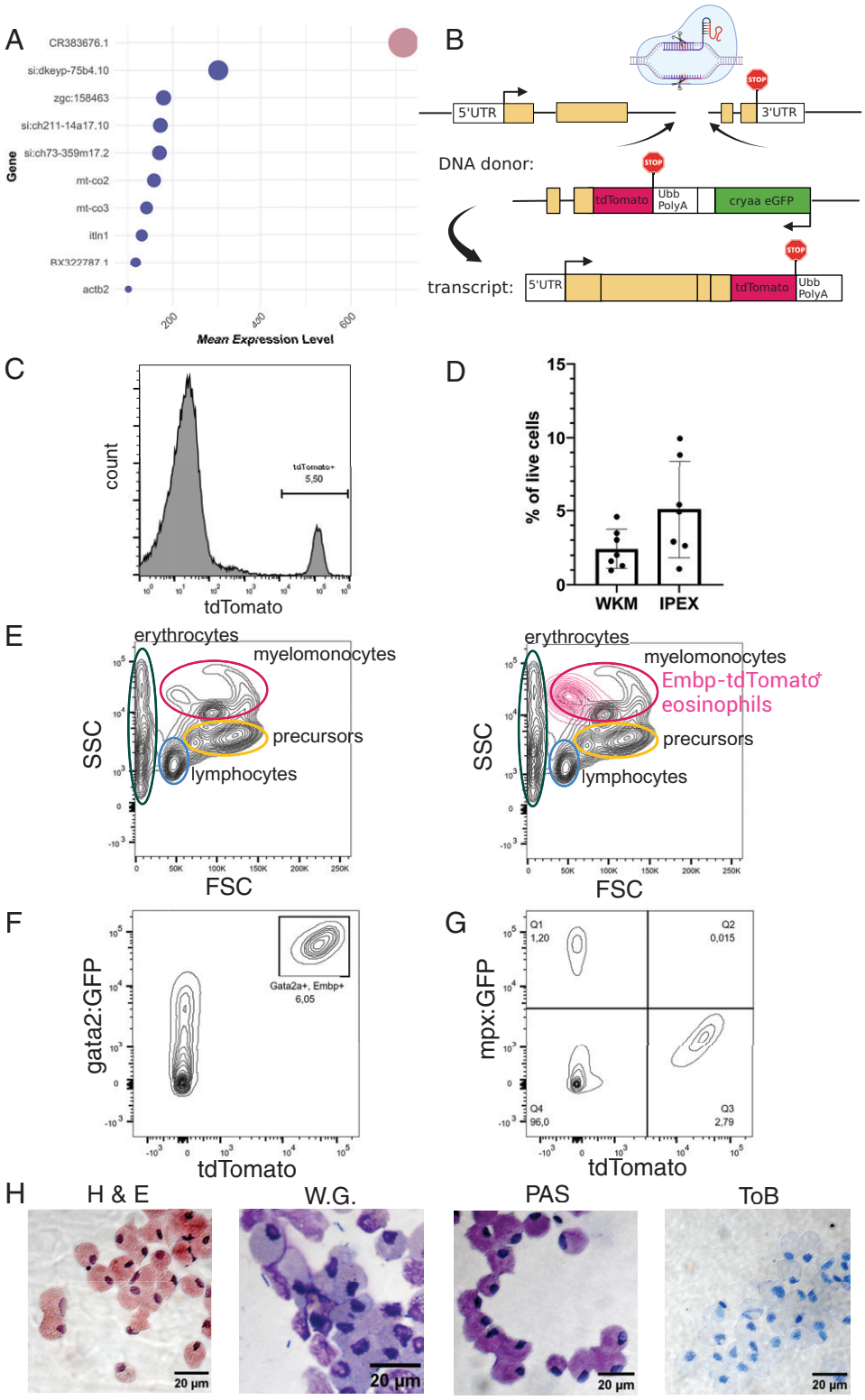

FIGURE 1. Generation of *TgKI(embp-tdTomato,cryaa:EGFP)* transgenic reporter line and initial validation. (**A**) Top 10 most highly expressed transcripts in the eosinophil population of dataset GSE161712 with color-coded information if they are protein coding. Bubble size refers to mean expression levels, and dark blue color indicates protein coding transcripts. (**B**) Schematic of genetic locus and DNA donor fragment inserted in the *embp* locus. Transcription leads to a fusion construct of Embp and tdTomato. (**C**) tdTomato expression in all live, single cells of a representative IPEX sample. (**D**) Quantification of Embp-tdTomato$^+$ cells in whole kidney marrow (WKM) and i.p. exudate (IPEX) samples of this transgenic line, measured by flow cytometry, and presentation as a proportion of live cells: WKM 2.4 ± 0.38% and IPEX 5.1 ± 2.7% (mean with SD). $n = 7$. (**E**) Traditional gating scheme by light-scatter characteristics of a representative WKM sample as previously reported (26). Side-by-side visualization with the Embp-tdTomato$^+$ cell population backgated onto the entire WKM in forward scatter (FSC)/side scatter (SSC). (**F**) Visualization of Embp-tdTomato and GFP driven by the *gata2a* promoter in a *TgKI(embp-tdTomato, cryaa:EGFP;gata2a:GFP)* double transgenic line. $n = 3$. (**G**) Visualization of Embp-tdTomato and GFP driven by the neutrophil promoter *mpx* in a *TgKI(embp-tdTomato,cryaa:EGFP; mpx:GFP)* double transgenic line. $n = 3$. (**H**) FACS-sorted Embp-tdTomato$^+$ cells stained with H&E, Wright–Giemsa (WG), periodic acid–Schiff (PAS), and toluidine blue (ToB). $n = 3$.

Our aim was to create a transgenic reporter line with a precise knock-in at the endogenous gene locus using CRISPR/Cas. By tagging the C terminus of Embp with a fluorescent protein, this approach will result in the generation of a full-length, tagged version of the protein under the control of the endogenous promoter, allowing us to visualize both eosinophils, and the localization of the Embp protein itself. A donor vector was designed (Fig. 1B) to generate this transgenic line. Next, a single-guide RNA was designed to create a double-strand break with CRISPR/Cas9 at the before-last intron of *embp*. The donor DNA fragment reconstitutes the remaining intronic sequence as well as the two last exons downstream of the cut site upon integration. Furthermore, it introduces a tdTomato sequence as a 3′ tag of our gene of interest, followed by a poly(A) sequence. The construct also includes a transgenesis marker using an eye-specific *cryaa* promoter to drive eGFP, enabling facile identification of embryos carrying this transgene prior to the emergence of eosinophils by bright green fluorescence in the lens.

Wild-type zebrafish eggs were injected at the one cell stage, screened for cryaa:GFP expression at 3 dpf, and raised to adulthood. F_0 founders were spawned and screened to identify founders transmitting the cryaa:GFP phenotype. cryaa:GFP-positive adult F_1 offspring (3–6 mo) with stable integration of the transgene were analyzed using flow cytometry for tdTomato expression in the granulocyte compartment. In zebrafish, eosinophils are commonly isolated from two sites: WKM, the bone marrow equivalent of zebrafish, and IPEX, cells collected from the peritoneal cavity. tdTomato$^+$ cells were identified within both WKM and IPEX populations (Fig. 1C). These tdTomato$^+$ cells were brightly fluorescent and appeared within the expected myelomonocytic gate using forward scatter/side scatter gating as has previously been done in zebrafish (26) (Fig. 1E). The proportions of tdTomato$^+$ cells in WKM (2.4 ± 0.38%) and IPEX (5.1 ± 2.7%) (Fig. 1D) corresponded well with the proportions of eosinophils observed in previous studies with Gata2a^{high} cells. To confirm the overlap with the previously used *Tg*(*gata2:eGFP*) line, *TgKI*(*embp-tdTomato,cryaa:EGFP*) fish were crossed with gata2a:GFP fish to generate a double transgenic line. The offspring were sorted for double-positive fluorescence at 3 dpf and analyzed in flow cytometry at 2 mo of age. As expected, the Embp-tdTomato$^+$ cells overlap with Gata2a^{high} cells, which have been previously described to be eosinophils (Fig. 1F), supporting the specificity of this reporter. We also identified a gata2a:GFP^{low} population of cells, which was found to be other noneosinophil myeloid populations in previous work (Fig. 1F), and this population is negative for Embp-tdTomato, suggesting that the Embp reporter is specific for eosinophils. To further confirm whether our reporter is specific for eosinophils, we assessed overlap of Embp reporter expression with neutrophil populations, as neutrophils are close relatives of eosinophils and undergo many of the same cellular processes as eosinophils (27, 28). Using the neutrophil marker *Tg*(*mpx:GFP*), we made double-transgenic *TgKI*(*embp-tdTomato,cryaa:EGFP*);*Tg*(*mpx:GFP*) animals. Flow cytometry of WKM and IPEX samples from these animals demonstrated that there was no overlap between Embp-tdTomato-expressing and mpx:GFP-expressing populations, supporting the specificity of our eosinophil-specific reporter (Fig. 1G).

As a final test of specificity, we isolated tdTomato$^+$ cells from *TgKI*(*embp-tdTomato,cryaa:EGFP*) and stained these populations with a panel of histological stains to corroborate the identity of the isolated cells. Using H&E, Wright–Giemsa (WG), and periodic acid–Schiff (PAS) staining, we found that tdTomato$^+$ cells showed the histological hallmarks of zebrafish eosinophils including a "round to oval shaped nucleus typically located peripherally" (11) (Fig. 1H). Importantly, both WG and H&E staining showed a uniform population of cells, and no cells were observed that showed the morphology of other immune lineages. Furthermore, we specifically investigated these isolated Embp-tdTomato$^+$ populations for the presence of mast cells, another highly granular immune population that has morphological similarity to eosinophils. Using the mast cell stain toludine blue (ToB), which has previously been shown to also identify mast cells in zebrafish (29), we found that Embp-tdTomato$^+$ populations were negative for ToB staining, which, together with our previous data, suggests that this reporter is highly specific. Confocal imaging of transgenic tdTomato$^+$ eosinophils isolated from *TgKI*(*embp-tdTomato,cryaa:EGFP*)^{ber1} animals revealed brightly fluorescent cells with the tagged transgene having a punctate localization that is consistent with targeting of this gene to the granules (Fig. 2A). This transgenic reporter could be visualized not only in isolated cell populations, but could also be used to observe eosinophil localization in formalin-fixed, paraffin-embedded (FFPE) sections in conjunction with a commercial mCherry Ab (Fig. 2B, Table I). Using immunofluorescence and histological staining of adjacent sections, we found that these tdTomato$^+$ transgenic eosinophils localized to the same sites in the zebrafish as their wild-type counterparts under homeostasis and possessed the histological characteristics of zebrafish eosinophils, suggesting that our tagging approach did not impact eosinophil homeostasis.

In conclusion, endogenous tagging of *embp* with tdTomato created a transgenic reporter line that enabled us to isolate and visualize zebrafish eosinophils. The transgenically tagged cells showed eosinophil morphology and characteristics by flow cytometry, histological staining, and confocal microscopy. Additionally, staining tissue sections with an mCherry Ab confirmed that tdTomato$^+$ eosinophils localize similar to their wild-type counterparts under homeostatic conditions, demonstrating that this targeting approach did not alter eosinophil localization in homeostasis. Furthermore, using this reporter line, we found that this transgene appeared to localize to granules, suggesting that Embp may be one member of the limited subset of eosinophil granular proteins.

Visualizing Embp-tdTomato$^+$ eosinophils and wild-type Embp both in situ and ex vivo

While our transgenic reporter line was useful to isolate eosinophils and visualize eosinophils in vivo, we also sought to establish a solution to visualize eosinophils in tissue samples that lack the transgenic reporter. To this end, we generated a custom polyclonal Ab targeting Embp (Fig. 3A). To confirm eosinophil specificity, the Ab was tested on WKM, IPEX, and isolated eosinophils of both *Tg*(*gata2:eGFP*) and *TgKI*(*embp-tdTomato,cryaa:EGFP*) lines (Fig. 3B, 3C). Positive staining was observed in 92.45/87.47% (Embp/Gata2a line) of sorted eosinophils, 4.62/3.58% (Embp/Gata2a line) of cells in WKM, and 12.63/9.86% (Embp/Gata2a line) of cells in IPEX samples, consistent with previous reports on the proportion of eosinophils in such samples. Importantly, staining of GFP$^-$ and tdTomato$^-$ fractions from *Tg*(*Gata2a:GFP*) or *TgKI*(*embp-tdTomato,cryaa:EGFP*) revealed no staining in eosinophil-depleted fractions by the Ab, highlighting its specificity (Supplemental Fig. 1B).

We also sought to determine whether this Ab could also be used to identify eosinophils in paraffin-embedded tissues. Ab staining of FFPE tissue sections (Fig. 4) demonstrated that this Ab could detect eosinophils within the tissue, with the staining patterns corresponding with the expected distribution of eosinophils within the tissue. To further corroborate stained cells as eosinophils, we stained adjacent sections with H&E and PAS (Fig. 4A), confirming that cells positive for Embp staining localized to the same locations as eosinophils detected by H&E and PAS. Eosinophils were found mainly in clusters in between organs of the peritoneal cavity, along the basal lamina propria in the gut and intestine, as well as in the WKM (Fig. 4B). Negligible Ab staining was observed in regions of the animal where few if any eosinophils were observed, confirming

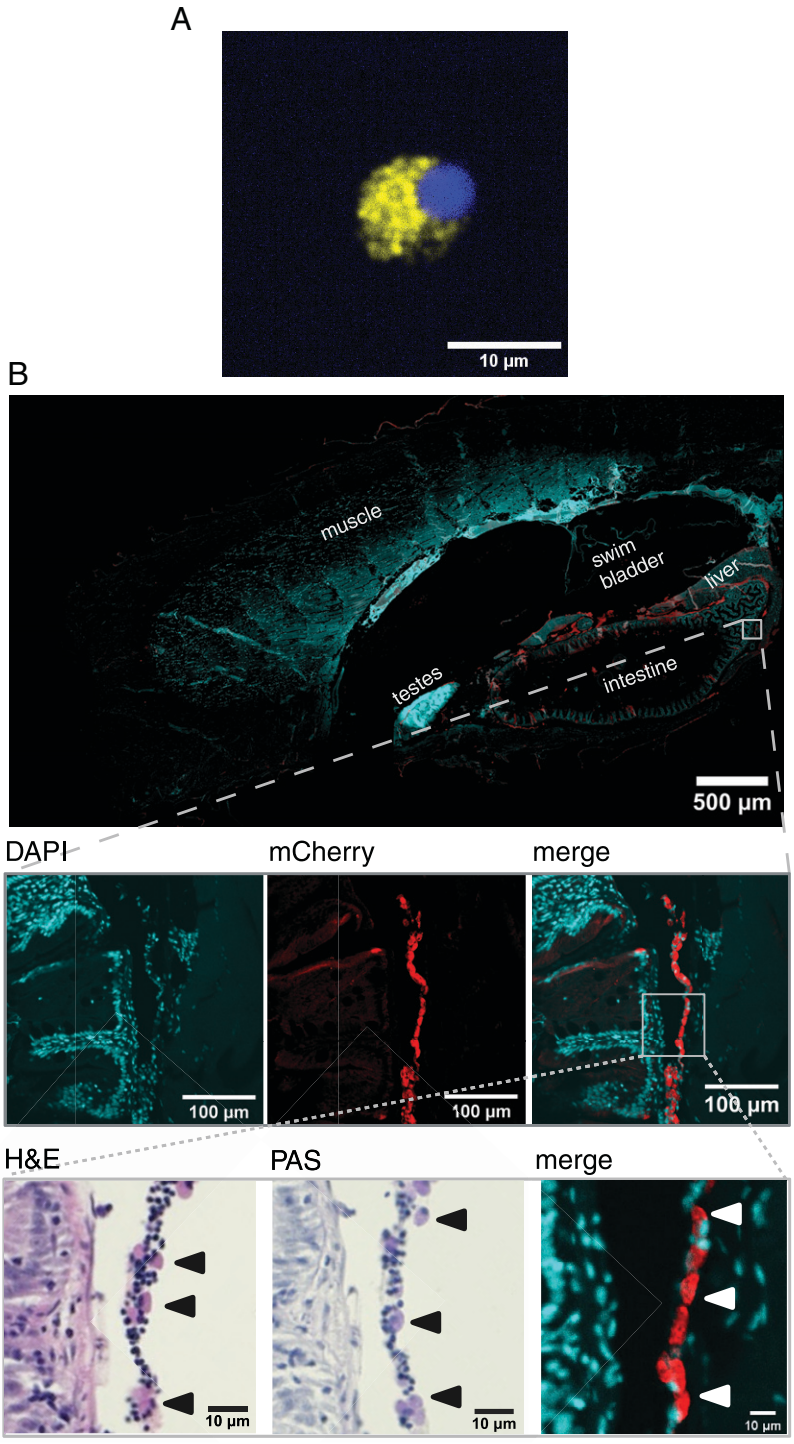

FIGURE 2. Confocal fluorescence microscopy of *TgKI*(*embp-tdTomato,cryaa:EGFP*) samples. (**A**) Imaging of a FACS isolated Embp-tdTomato^{+} (yellow) eosinophil. The fluorescent transgene is localized within likely eosinophil granula. Nuclear counterstain with DAPI. (**B**) Detection of the Embp-tdTomato transgene in 5-µm FFPE sections using an mCherry Ab. Eosinophils are found along the lamina propria lining the intestine and between organs, confirmed by H&E and PAS staining of adjacent sections.

the specificity of the Ab binding and efficacy of this reagent for the detection of endogenous eosinophils.

During inflammation, immune populations including eosinophils undergo profound transcriptional changes and eosinophils can also undergo degranulation, processes that can shift reporter gene expression and localization. To confirm that our Ab and the broader reporter approach could still be used to detect eosinophils within inflamed tissues, we visualized eosinophil localization in *M. marinum*–infected FFPE samples of adult zebrafish (Fig. 4C). *M. marinum* infection causes granulomatous inflammation in zebrafish, and eosinophils have been found within the zebrafish granuloma (30). We found that eosinophils could be stained within the mycobacterial granuloma as well as in surrounding tissue, indicating that even under inflamed conditions, this marker could be used to identify eosinophils. This finding is also consistent with previous studies demonstrating recruitment of eosinophils to mycobacterial granulomas, providing further evidence for eosinophils within this structure and the spatial distribution of the cells throughout the granuloma.

Our previous experiments have indicated that not only is Embp an effective marker of eosinophils, but they have also supported a putative eosinophil granular localization for Embp. In mammals, eosinophil granules contain a limited array of highly expressed effector genes. To definitively establish Embp as a granular protein, we employed cryo-immunogold EM to localize Embp within

Table I. Abs used in this study

Ab	Source	Identifier
E-cadherin clone 36	BD Transduction Laboratories	610181
dkeyp75b4.10	Boster Bio	DZ41383
GFP	Aves Labs	GFP-1020
mCherry	Aves Labs	MCHERRY-0100
Alexa Fluor 647 goat anti-mouse	Thermo Fisher Scientific	A-21235
Alexa Fluor 555 goat anti-rabbit	Invitrogen	A32732
Alexa Fluor 647 goat anti-rabbit	Invitrogen	A32733
Alexa Fluor 488 goat anti-chicken IgY	Thermo Fisher Scientific	A-11039
Alexa Fluor 647 Goat anti-chicken IgY	Thermo Fisher Scientific	A-32933
6-nm colloidal gold goat anti-chicken IgY	Jackson ImmunoResearch	103-005-155
12-nm colloidal gold goat anti-rabbit	Jackson ImmunoResearch	111-205-144

the eosinophil. Embp-tdTomato^{+} eosinophils were isolated from *TgKI*(*embp-tdTomato,cryaa:EGFP*) animals by flow cytometry and stained with both our polyclonal Embp Ab, to detect the native Ag, and an mCherry Ab, to visualize transgene localization within the same cells. We found that both the endogenous Embp and the tdTomato transgene are almost entirely localized within the granules of the eosinophils, with only sporadic protein detection in the cytoplasm (Fig. 5). Thus, our findings establish Embp as a bona fide eosinophil granular protein in zebrafish, and demonstrate a potential role for this protein as an eosinophil effector protein.

Discussion

Eosinophils are critical effectors of the vertebrate immune response, contributing to the control of helminth pathogens and tissue remodeling but also leading to detrimental pathology in diseases such as

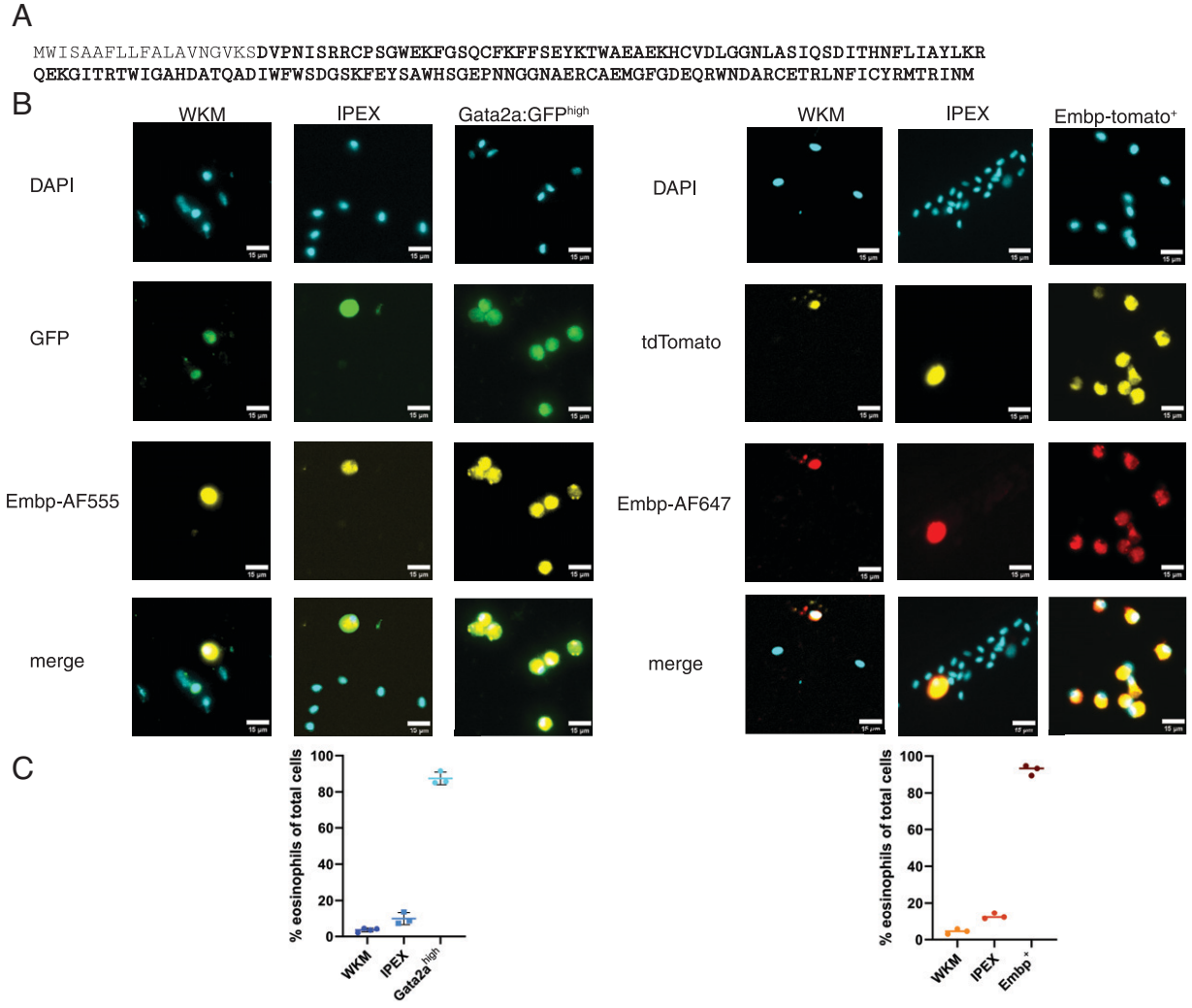

FIGURE 3. Immunofluorescence staining with a novel polyclonal Ab targeting Embp. (**A**) Amino acid sequence of Embp in single letter code demonstrating in bold the part of the Ag used to generate the polyclonal Ab. (**B**) Staining of isolated WKM, IPEX, and eosinophil cell populations of both the *Tg*(*gata2:eGFP*) and *TgKI*(*embp-tdTomato,cryaa:EGFP*) lines. Eosinophils were sorted by transgenic reporter expression (either Gata2a^{high} or Embp^{+}). $n = 3$. (**C**) Quantification of cells stained positively for Embp with polyclonal Ab in the aforementioned sorted cell populations. Positive staining was assessed in a minimum of six random fields of view across three independent experiments; 300–500 cells were evaluated per sample. Data are represented as percentage of positive Embp staining in total cell population, including mean with SD of each independent experiment.

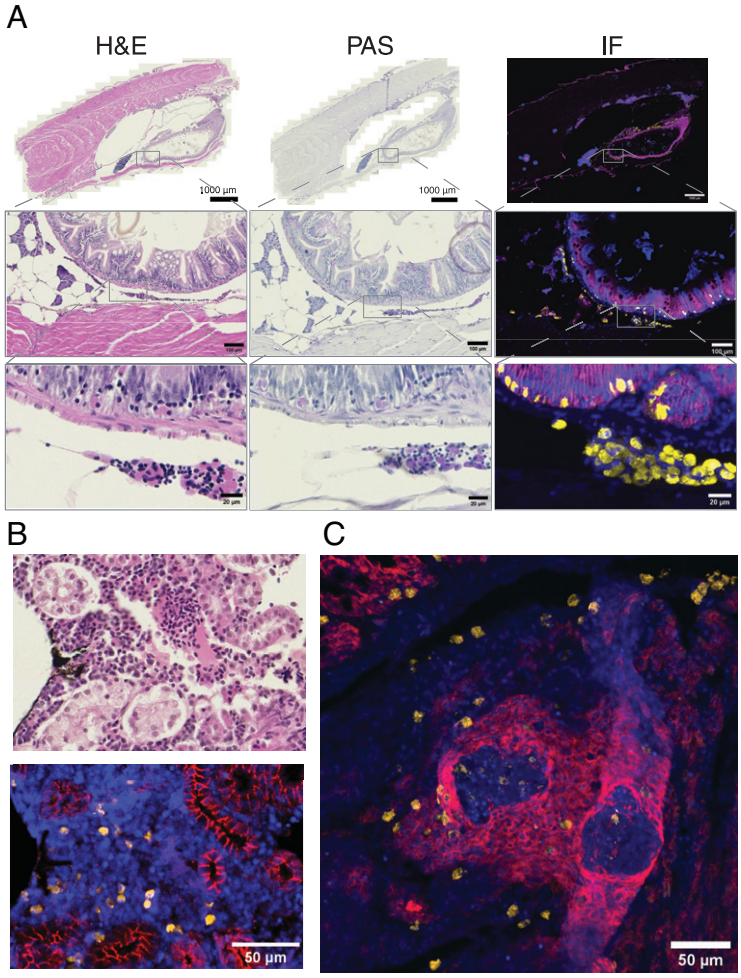

FIGURE 4. Embp Ab staining in FFPE tissue samples. (**A**) H&E, PAS, and immunofluorescence (IF) staining with Embp Ab in healthy *TgKI*(*embp-tdTomato,cryaa:EGFP*) adults. Blue indicates DAPI; yellow indicates eosinophils; magenta indicates E-cadherin staining of epithelial cells. $n = 3$. (**B**) Zoom in on a part of the WKM, showing the Embp^{+} stain in this tissue together with the corresponding site in H&E staining of the adjacent section. Same IF staining as in (A). (**C**) Staining of eosinophils in *M. marinum*–infected zebrafish FFPE sections. Eosinophils can be found in physiological sites in the body as well as in granuloma. Magenta indicates E-cadherin, marking epithelioid macrophages surrounding the necrotic core of the granuloma; yellow indicates eosinophils stained by Embp Ab; blue indicates DAPI.

asthma (9). Eosinophils are broadly conserved in vertebrates, but despite their recognition in zebrafish (11), tools to study this cell population and their specialized effectors are lacking in this emerging infection model. In this study, we identified, a highly specific marker for zebrafish eosinophil granules, Embp. We initially identified Embp from analysis of previously published RNA sequencing datasets, which suggested that *embp* (also known as *dkeyp75b4.10* ENSDART00000143719, ENSDART00000110749) was both highly and differentially expressed in eosinophilic granulocytes, with minimal expression in other hematopoietic-derived lineages (23). Among the transcripts expressed within the eosinophil population, *embp* was identified as the most highly expressed protein coding transcript, with the sole RNA expressed at higher levels being CR383676.1, a small noncoding RNA of unknown function. This eosinophil-specific expression of Embp is consistent with recent observations of this gene and its promoter (26), although the localization and function of this gene were unclear. We generated a transgenic reporter line tagging the endogenous Embp with a fluorescent protein on its 3′ end by CRISPR insertion to investigate the localization of this gene, resulting in the endogenous promoter of *embp* driving the expression of a full-length transgenic Embp-tdTomato construct. Using this zebrafish line, we found that *embp* was specifically expressed within eosinophils and not in other immune populations, demonstrating that this line could be used to specifically mark eosinophils in zebrafish. This marker line could be used for flow cytometry, confocal microscopy, and histochemistry to identity eosinophils, expanding the toolkit available to study the function of these cells in zebrafish. In addition, a newly generated polyclonal Ab targeting Embp allows visualization of endogenous eosinophils in vivo and ex vivo.

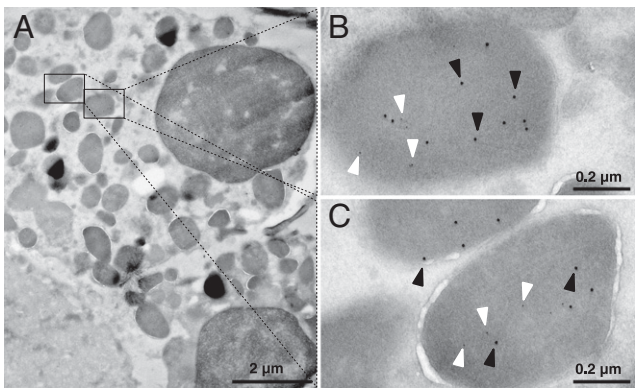

FIGURE 5. Cryo-immunogold EM of FACS isolated Embp-tdTomato^{+} eosinophils. (**A**) Overview of an eosinophil. (**B** and **C**) Zoom in on two different granula of this cell. Embp Ab is visualized by a 12-nm gold secondary Ab (black arrowheads) and mCherry Ab is visualized by 6-nm gold secondary Ab (white arrowheads). Both target Ags were detected in the same granule.

Comparing the proportions of eosinophils in the previously characterized *Tg*(*gata2:eGFP*) line and our new *TgKI*(*embp-tdTomato, cryaa:EGFP*) line, we find very similar levels of our cells of interest. Although numbers were close between the two lines, we did find a slight statistically significant increase in the number of eosinophils only in the WKM population of *TgKI*(*embp-tdTomato,cryaa:EGFP*) (Supplemental Fig. 1A) but not in IPEX

populations. Considering the low number of eosinophils in WKM and the high variability in eosinophil number per animal in our data and the data of other groups (11), we expect that this could potentially be driven by stochastic differences in this small group of animals. A second possibility is that the distinct fluorophores and fluorescence intensity of each reporter could lead to subtle differences in the detection frequency. Overall, however, the relative number of eosinophils in the new *TgKI(embp-tdTomato,cryaa:EGFP)* reporter line falls within the range of previously reported eosinophil counts (11).

Structurally, Embp possesses a C-type lectin domain. Although there are a number of C-type lectin proteins expressed in mammalian eosinophils, including major basic protein 1 (MBP-1) (31), major basic protein 2 (MBP-2) (32), Dectin-1 (33) and C-type lectin domain family 4, member a4 (Clec4a4) (34), MBP-1 and MBP-2 are the only C-type lectins that are canonical granule proteins in mammalian eosinophils (8). Our cryo-EM data (Fig. 5), together with confocal microscopy (Fig. 2), demonstrate that in zebrafish Embp is an eosinophil granule protein, likely acting as an eosinophil effector molecule. MBP-1 and MBP-2 are among the most highly expressed proteins in mammalian eosinophils. Similarly, *embp* was identified as the most highly expressed protein-coding gene in single-cell RNA sequencing data, and both our reporter and Ab show robust positivity, suggesting a high level of expression. Based on the strong expression of Embp, the localization within the granules, its exclusivity to eosinophils, and its C-type lectin domain, one possibility is that Embp could be a zebrafish ortholog of the MBP family.

In mammals, eosinophil MBP-1 is, as the name suggests, characterized by a strongly basic isoelectric point (pI). Surprisingly, the pI of Embp is relatively neutral (pI 6.8), suggesting that either Embp is not the true ortholog of human (h)MBP-1 or that the strongly basic character of hMBP-1 is an evolutionarily recent change. Whereas hMBP-1 is highly basic (pI 11.4), hMBP-2 is known to also have a pI much closer to neutral (pI 8.7). Additionally, the pIs of MBP orthologs vary considerably across species (32, 35). As we saw in zebrafish for Embp, hMBP-2 is exclusively expressed in eosinophils (32), whereas hMBP-1, although predominantly expressed in eosinophils, is also expressed in basophils and mast cells, suggesting that if Embp is an MBP family ortholog, it may be the ortholog of hMBP-2. Interestingly, in ruminants, MBP-2 is the only MBP present (35). Further studies into the biochemical and functional properties of Embp are needed to determine whether this gene is a member of the MBP protein family, but if this is the case, zebrafish Embp may offer an interesting window into the evolution of MBP proteins.

Addressing a critical gap in the study of zebrafish eosinophils, the new tools presented in this study will allow the study of the development and maturation of eosinophils as well as the function of eosinophils in diverse diseases. Recent efforts using zebrafish to model allergic inflammation and food allergies have identified granulocytes as significant contributors to these conditions (36), but they have not been able to identify the specific cell types responsible. By facilitating studies of eosinophil function in zebrafish, our tools will enable researchers to discover new roles for eosinophils that can be conserved in human disease. The similarities and differences in eosinophil responses in zebrafish will also offer a window into the evolution of these cells, as zebrafish are one of the most distant human ancestors to have eosinophils. Use of zebrafish for comparative immunology approaches will highlight centrally conserved immune responses and eosinophil behavior that function across vertebrate species.

Acknowledgments

We thank the Zychlinsky department for sharing lab equipment and reagents as well as helpful discussion. We thank Charlie J. Pyle and David M. Tobin for sharing material and Silke Lehmann, Marten Walk, Carsten Weiland, Janine Bleske, Jens Otto and Ines Neumann for excellent care of the zebrafish facility. Figures were created using BioRender.com.

Disclosures

The authors have no financial conflicts of interest.

References

1. Cronan, M. R., and D. M. Tobin. 2014. Fit for consumption: zebrafish as a model for tuberculosis. *Dis. Model. Mech.* 7: 777–784.
2. White, R. M., and E. E. Patton. 2023. Adult zebrafish as advanced models of human disease. *Dis. Model. Mech.* 16: dmm050351.
3. Santoriello, C., and L. I. Zon. 2012. Hooked! Modeling human disease in zebrafish. *J. Clin. Invest.* 122: 2337–2343.
4. Renshaw, S. A., and N. S. Trede. 2012. A model 450 million years in the making: zebrafish and vertebrate immunity. *Dis. Model. Mech.* 5: 38–47.
5. Carradice, D., and G. J. Lieschke. 2008. Zebrafish in hematology: sushi or science? *Blood* 111: 3331–3342.
6. Zizioli, D., M. Mione, M. Varinelli, M. Malagola, S. Bernardi, E. Alghisi, G. Borsani, D. Finazzi, E. Monti, M. Presta, et al. 2019. Zebrafish disease models in hematology: Highlights on biological and translational impact. *Biochim. Biophys. Acta Mol. Basis Dis.* 1865: 620–633.
7. Ehrlich, P. 1877. Beiträge zur Kenntniss der Anilinfärbungen und ihrer Verwendung in der mikroskopischen Technik. *Archiv f. Mikrosk. Anat.* 13: 263–277.
8. Lee, J. J., and H. F. Rosenberg, eds. 2013. *Eosinophils in Health and Disease.* London: Academic Press.
9. Chusid, M. J. 2018. Eosinophils: friends or foes? *J. Allergy Clin. Immunol. Pract.* 6: 1439–1444.
10. Mayer-Barber, K. D. 2023. Granulocytes subsets and their divergent functions in host resistance to Mycobacterium tuberculosis—a "tipping-point" model of disease exacerbation. *Curr. Opin. Immunol.* 84: 102365.
11. Balla, K. M., G. Lugo-Villarino, J. M. Spitsbergen, D. L. Stachura, Y. Hu, K. Bañuelos, O. Romo-Fewell, R. V. Aroian, and D. Traver. 2010. Eosinophils in the zebrafish: prospective isolation, characterization, and eosinophilia induction by helminth determinants. *Blood* 116: 3944–3954.
12. Meng, A., H. Tang, B. A. Ong, M. J. Farrell, and S. Lin. 1997. Promoter analysis in living zebrafish embryos identifies a cis-acting motif required for neuronal expression of GATA-2. *Proc. Natl. Acad. Sci. USA* 94: 6267–6272.
13. Mathias, J. R., B. J. Perrin, T.-X. Liu, J. Kanki, A. T. Look, and A. Huttenlocher. 2006. Resolution of inflammation by retrograde chemotaxis of neutrophils in transgenic zebrafish. *J. Leukoc. Biol.* 80: 1281–1288.
14. Levic, D. S., N. Yamaguchi, S. Wang, H. Knaut, and M. Bagnat. 2021. Knock-in tagging in zebrafish facilitated by insertion into non-coding regions. *Development* 148: dev199994.
15. Engler, C., R. Gruetzner, R. Kandzia, and S. Marillonnet. 2009. Golden gate shuffling: a one-pot DNA shuffling method based on type IIs restriction enzymes. *PLoS One* 4: e5553.
16. Kurita, R., H. Sagara, Y. Aoki, B. A. Link, K. I. Arai, and S. Watanabe. 2003. Suppression of lens growth by αA-crystallin promoter-driven expression of diphtheria toxin results in disruption of retinal cell organization in zebrafish. *Dev. Biol.* 255: 113–127.
17. Svoboda, O., D. L. Stachura, O. Machonova, L. I. Zon, D. Traver, and P. Bartunek. 2016. Ex vivo tools for the clonal analysis of zebrafish hematopoiesis. *Nat. Protoc.* 11: 1007–1020.
18. Copper, J. E., L. R. Budgeon, C. A. Foutz, D. B. van Rossum, D. J. Vanselow, M. J. Hubley, D. P. Clark, D. T. Mandrell, and K. C. Cheng. 2018. Comparative analysis of fixation and embedding techniques for optimized histological preparation of zebrafish. *Comp. Biochem. Physiol. C Toxicol. Pharmacol.* 208: 38–46.
19. Schindelin, J., I. Arganda-Carreras, E. Frise, V. Kaynig, M. Longair, T. Pietzsch, S. Preibisch, C. Rueden, S. Saalfeld, B. Schmid, et al. 2012. Fiji: an open-source platform for biological-image analysis. *Nat. Methods* 9: 676–682.
20. Peters, P. J., E. Bos, and A. Griekspoor. 2006. Cryo-immunogold electron microscopy. *Curr. Protoc. Cell Biol.* Chapter 4:Unite 4.7.
21. Slot, J. W., H. J. Geuze, S. Gigengack, G. E. Lienhard, and D. E. James. 1991. Immuno-localization of the insulin regulatable glucose transporter in brown adipose tissue of the rat. *J. Cell Biol.* 113: 123–135.
22. Mutterer, J., and E. Zinck. 2013. Quick-and-clean article figures with FigureJ. *J. Microsc.* 252: 89–91.
23. Cronan, M. R., E. J. Hughes, W. J. Brewer, G. Viswanathan, E. G. Hunt, B. Singh, S. Mehra, S. H. Oehlers, S. G. Gregory, D. Kaushal, et al. 2021. A non-canonical type 2 immune response coordinates tuberculous granuloma formation and epithelialization. *Cell* 184: 1757–1774.e14.
24. Baron, C. S., A. Barve, M. J. Muraro, R. van der Linden, G. Dharmadhikari, A. Lyubimova, E. J. P. de Koning, and A. van Oudenaarden. 2019. Cell type purification by single-cell transcriptome-trained sorting. *Cell* 179: 527–542.e19.

25. Li, G., Y. Sun, I. Kwok, L. Yang, W. Wen, P. Huang, M. Wu, J. Li, Z. Huang, Z. Liu, et al. 2024. Cebp1 and Cebpβ transcriptional axis controls eosinophilopoiesis in zebrafish. *Nat. Commun.* 15: 811.
26. Traver, D., B. H. Paw, K. D. Poss, W. T. Penberthy, S. Lin, and L. I. Zon. 2003. Transplantation and in vivo imaging of multilineage engraftment in zebrafish bloodless mutants. *Nat. Immunol.* 4: 1238–1246.
27. Kobayashi, T., E. Garcia Del Saz, J. Hendry, and H. Seguchi. 1999. Detection of oxidant producing-sites in glutaraldehyde-fixed human neutrophils and eosinophils stimulated with phorbol myristate acetate. *Histochem. J.* 31: 181–194.
28. Berdnikovs, S. 2021. The twilight zone: plasticity and mixed ontogeny of neutrophil and eosinophil granulocyte subsets. *Semin. Immunopathol.* 43: 337–346.
29. Dobson, J. T., J. Seibert, E. M. Teh, S. Da'as, R. B. Fraser, B. H. Paw, T.-J. Lin, and J. N. Berman. 2008. Carboxypeptidase A5 identifies a novel mast cell lineage in the zebrafish providing new insight into mast cell fate determination. *Blood* 112: 2969–2972.
30. Bohrer, A. C., E. Castro, Z. Hu, A. T. L. Queiroz, C. E. Tocheny, M. Assmann, S. Sakai, C. Nelson, P. J. Baker, H. Ma, et al. Tuberculosis Imaging Program. 2021. Eosinophils are part of the granulocyte response in tuberculosis and promote host resistance in mice. *J. Exp. Med.* 218: e20210469.
31. Swaminathan, G. J., D. G. Myszka, P. S. Katsamba, L. E. Ohnuki, G. J. Gleich, and K. R. Acharya. 2005. Eosinophil-granule major basic protein, a C-type lectin, binds heparin. *Biochemistry* 44: 14152–14158.
32. Plager, D. A., D. A. Loegering, J. L. Checkel, et al. 2006. Major basic protein homolog (MBP2): a specific human eosinophil marker. *J. Immunol.* 177: 7340–7345.
33. Kerrigan, A. M., and G. D. Brown. 2009. C-type lectins and phagocytosis. *Immunobiology* 214: 562–575.
34. Wang, W.-L., J. Kasamatsu, S. Joshita, S. Gilfillan, B. Di Luccia, S. K. Panda, D.-H. Kim, P. Desai, J. K. Bando, S. C.-C. Huang, et al. 2022. The aryl hydrocarbon receptor instructs the immunomodulatory profile of a subset of Clec4a4^{+} eosinophils unique to the small intestine. *Proc. Natl. Acad. Sci. USA* 119: e2204557119.
35. Jenvey, C. J., D. Alenizi, F. Almasi, C. Cairns, A. Holmes, S. Sloan, and M. J. Stear. 2020. Bioinformatic analysis of eosinophil activity and its implications for model and target species. *Parasitology.* 147: 393–400.
36. Contreras, M., I. Pacheco, P. Alberdi, S. Díaz-Sánchez, S. Artigas-Jerónimo, L. Mateos-Hernández, M. Villar, A. Cabezas-Cruz, and J. de la Fuente. 2020. Allergic reactions and immunity in response to tick salivary biogenic substances and red meat consumption in the zebrafish model. *Front. Cell. Infect. Microbiol.* 10: 526483.